Contrasting Nodal and Anti-Nodal Behavior in the Cuprates Via Multiple Gap Spectroscopies

Dan Wulin[1], Chih-Chun Chien[1], Dirk K. Morr[1,2] and K. Levin[1]

[1] *James Frank Institute and Department of Physics, University of Chicago, Chicago, Illinois 60637*
[2] *Department of Physics, University of Illinois at Chicago, Chicago, Illinois 60607*

(Dated: December 15, 2009)

Using a precursor superconductivity scenario for the cuprates we present a theory for the temperature dependent behavior of the spectral gaps associated with four distinct spectroscopies: angle resolved photoemission (ARPES), differential conductance dI/dV, quasi-particle interference spectroscopy, and the autocorrelated ARPES pattern. We find good agreement for a range of existing experiments and make predictions for others. Our theory, which incorporates the necessary (observed) contrast between the nodal and anti-nodal response, shows how different nodal gap shapes are associated with these alternative spectroscopies.

PACS numbers: 74.25.Jb, 74.20.-z, 74.72.-h

arXiv:0912.3008v1 [cond-mat.supr-con] 15 Dec 2009

A central focus in current studies of high temperature superconductivity is on establishing the origin of the pseudogap. The various theoretical scenarios that have been put forth can be broadly categorized into two schools of thought that either relate the pseudogap to superconductivity through precursor pairing or ascribe its origin to a new and competing form of order[1]. Important constraints for these scenarios have been provided by recent scanning tunneling microscopy (STM)[2,3,4] and angle-resolved photoemission spectroscopy (ARPES)[5,6] experiments, which have reported pronounced differences in the behavior of the spectral gap along the nodal and anti-nodal directions, and a deviation of the superconducting gap below T_c from the symmetry of a monotonic d-wave function (with the exception of the moderately underdoped cuprates at very low temperatures). Whether these observations are sufficient to rule out one of the above theoretical proposals for the origin of the pseudogap, as has been claimed[5,6], is currently unclear. The situation has been further complicated by an ongoing controversy about whether[7,8,9] or not[10] these various experimental probes yield the same spectral gap.

In this article, we address these issues by studying four different spectroscopic techniques using a single theoretical framework: the spectral function and the autocorrelated joint density of states (JDOS) derived from ARPES experiments, as well as the differential conductance, dI/dV, and quasi-particle interference spectroscopy, obtained from STM experiments. For each technique, we follow the experimental protocols to deduce the angular dependence of the associated spectral gap. Our theoretical framework is motivated by the idea that the anomalously short coherence length of the cuprate superconductors and the concomitant stronger-than-BCS attractive interactions can lead to preformed pairs above T_c as the origin of the pseudogap[11]. The results of our study are two-fold. *Firstly, we demonstrate that the robust and salient features of STM and ARPES experiments above and below T_c can be consistently explained within a preformed pair scenario*. In particular, we show that the superconducting gap deviates from the pure $d_{x^2-y^2}$-form, i.e., $(\cos k_x - \cos k_y)$, in the moderately underdoped cuprates. This deviation only occurs as the pseudogap state is approached near but below T_c, in agreement with experiment[4,12]. In the heavily underdoped cuprates, we show how this deviation occurs for all temperatures[13] below T_c. Moreover, we find that these ubiquitous deviations in gap shape are tied to the Fermi arcs[14] observed above T_c, which is consistent with recent experimental STM results[4]. *Secondly, we demonstrate that the superconducting gaps extracted from these different spectroscopies are only in good quantitative agreement in those parts of the phase diagram where the spectroscopic gap follows a $(\cos k_x - \cos k_y)$ form*. However, when the gap deviates from this form, the four spectroscopies can yield widely different results, particularly in the nodal region. These findings provide important insight into the question of consistency between different spectroscopic probes in the cuprate superconductors.

In the theoretical BCS-BEC crossover scenario considered here, the pseudogap arises from pre-formed pairs in the normal state, which become non-condensed pair excitations of the condensate below T_c. This scenario is consistent with the emerging physical picture[4,5,6] that pseudogap effects persist below T_c, which differentiates our model[11,15] from other approaches considering precursor pairing[1]. For the moderately underdoped systems, there are indications[6] that the ground state gap has conventional $d_{x^2-y^2}$ symmetry, which we presume here. As previously discussed[11,15], the condensed and non-condensed (or preformed) pairs yield two distinct contributions to the fermionic self energy, given by $\Sigma(K) = \Sigma_{sc}(K) + \Sigma_{pg}(K)$ with

$$\Sigma_{sc}(K) = \frac{\Delta^2_{sc}(\mathbf{k})}{\omega + \epsilon_k - \mu}; \quad \Sigma_{pg}(K) = \frac{\Delta^2_{pg}(\mathbf{k})}{\omega + \epsilon_k - \mu + i\gamma}. \tag{1}$$

Here K is a four-vector, and we define $\Delta^2(\mathbf{k}, T) \equiv \Delta^2_{sc}(\mathbf{k}, T) + \Delta^2_{pg}(\mathbf{k}, T)$. The momentum dependence for both Δ_{sc} and Δ_{pg} is given by the same pure $d_{x^2-y^2}$-wave form. The condensed pairs have the usual BCS self energy contribution, Σ_{sc}, while the self energy of the non-condensed pairs Σ_{pg} is similar except for an overall broadening factor γ. This form for Σ_{pg} has been widely accepted in the cuprate community, in particular, for the normal state[16].

The above framework provides a simple explanation for the different temperature dependencies of the nodal and anti-nodal spectral gap observed experimentally. Above T_c, the finite lifetime associated with the preformed pairs leads to a blurring of the d-wave gap near the nodes and thus to the for-

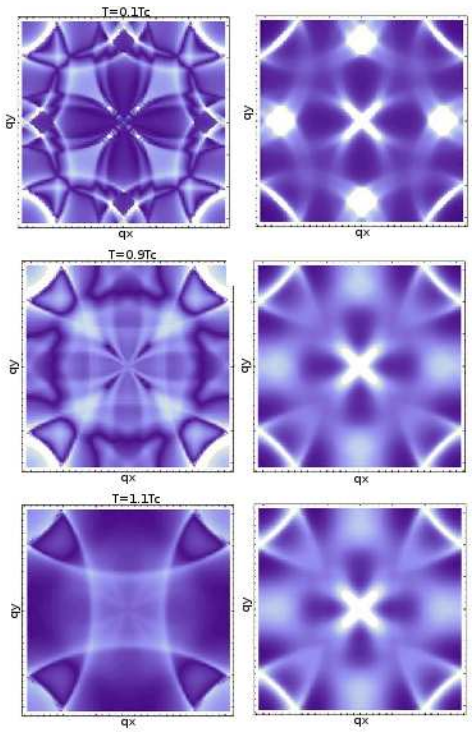

Figure 1: (Color online) Each column shows $\delta n(\mathbf{q},\omega)(J(\mathbf{q},\omega))$ for $\omega = -10meV$ and temperatures $T = 0.1, 0.9$, and $1.1T_c$. At low temperatures, δn shows well-defined octet peaks. With increasing temperature the octet peaks are broadened and vanish into the background for $T \geq T_c$. The wavevector $\mathbf{q}$ is in units of the inverse lattice constant.

mation of Fermi arcs[17]. At the anti-nodes, this effect of γ is inconsequential since the normal state gap, as described by Δ_{pg}, is large there. When the system passes below T_c the nodal region should be thought of as analogous to an ordinary BCS superconductor which has a gapless normal state and is, thus, profoundly sensitive to the onset of coherent order (via Δ_{sc}). The anti-nodal region, with its well developed normal state gap is, by contrast, rather insensitive to T_c.

We next turn to a discussion of the four different spectroscopic techniques mentioned above. In ARPES experiments, one measures the electronic spectral function $A(\mathbf{k},\omega) = -\frac{1}{\pi}\mathrm{Im}G(\mathbf{k},\omega)$, where $G(\mathbf{k},\omega)$ contains the self-energy corrections of Eq.(1). Derived from the spectral function is the joint density of states (JDOS), which is given by

$$J(\mathbf{q},\omega) \propto \int d^2k A(\mathbf{k}+\mathbf{q},\omega)A(\mathbf{k},\omega) \tag{2}$$

On the other hand, in STM experiments, one measures the differential conductance dI/dV, which is given by

$$\frac{dI}{dV}(V) \propto -\int d\omega f'(\omega - V)\int \frac{d^2k}{(2\pi)^2}A(\mathbf{k},\omega) \tag{3}$$

Here $f'(\omega)$ is the derivative of the Fermi distribution function. Finally, the STM-based quasi particle interference (QPI) spectroscopy investigates changes in the local density of states (LDOS) arising from impurity scattering[10]. For a single point-like impurity, the Fourier transform of the first order correction to the LDOS (i.e, the QPI intensity) is given by

$$\delta n(\mathbf{q},\omega) \propto -\mathrm{Im}\left[\int \frac{d^2k}{(2\pi)^2}\left(G(\mathbf{k},\omega)G(\mathbf{k}+\mathbf{q},\omega)\right.\right.$$
$$\left.\left.-F_{sc}(\mathbf{k},\omega)F_{sc}(\mathbf{k}+\mathbf{q},\omega) - F_{pg}(\mathbf{k},\omega)F_{pg}(\mathbf{k}+\mathbf{q},\omega)\right)\right] \tag{4}$$

where $F_{sc}(\mathbf{k},\omega) \equiv -\Delta_{sc,\mathbf{k}}G(\mathbf{k},\omega)/(\omega + \xi_{\mathbf{k}})$ and $F_{pg}(\mathbf{k},\omega) \equiv -\Delta_{pg,\mathbf{k}}G(\mathbf{k},\omega)/(\omega + \xi_{\mathbf{k}} + i\gamma)$. It is important to note that $J(\mathbf{q},\omega)$ and $\delta n(\mathbf{q},\omega)$ are two distinct physical quantities and thus not directly related, since the former is a convolution of ImG only, while the latter contains both the real and imaginary parts of G and F.

The deduction of the associated spectral gaps proceeds as follows. In ARPES experiments, we deduce a spectral gap from the peak to peak separation of the symmetrized spectral function[18]. The approach of extracting a gap from the differential conductance is outlined in Ref. 4, where the dI/dV curve is fitted with a sum of BCS-like gaps Δ_j with corresponding weights W_j, according to

$$\frac{dI}{dV}(V) \propto \int d\omega f'(\omega+V)\sum_j \mathrm{Re}\frac{\omega - i\Gamma}{\sqrt{(\omega - i\Gamma)^2 - \Delta_j^2}}W_j \tag{5}$$

The parameter Γ is used to fit the differential conductance at zero bias. Once the weights are obtained, they implicitly define the angular dependence of the gap, $\Delta(\Phi)$, from the inversion of $\Phi(\Delta = \Delta_j) \propto \sum_{i=1}^{j} W_i$.

The extraction of the spectral gaps both from $J(\mathbf{q},\omega)$ and $\delta n(\mathbf{q},\omega)$ assumes the validity of the octet model[2]. This model is based on the observation that, since the spectral function $A(\mathbf{k},\omega)$ is peaked at the tips of the contours of constant energy ω, the convolution of two spectral functions in $J(\mathbf{q},\omega)$ should exhibit peaks at those momenta $\mathbf{q}_i$ that connect the tips. The resulting dependence of $\mathbf{q}_i$ on energy, $\mathbf{q}_i(\omega = \Delta(\Phi))$, can then be inverted to obtain the momentum (or angular) dependence of the gap. While $\delta n(\mathbf{q},\omega)$ is not a convolution of two spectral functions, it has been suggested that a similar argument still holds. We anticipate that since the octet model is derived from considerations of $J(\mathbf{q},\omega)$, its related inversion procedure will yield a spectral gap closer to a pure d-wave form. In our extraction of the spectral gaps, we use the octet vectors $\mathbf{q}_1$ and $\mathbf{q}_5$, and $\mathbf{q}_3$ and $\mathbf{q}_7$. Each pair of vectors yields a different angle function $\Phi(\Delta)$ and we require for consistency of the octet model that the two angular functions differ by no more than 5%.

We start by discussing the spectral gaps in the moderately underdoped cuprates. In the first (second) column of Fig.1, we present contour plots of $\delta n(\mathbf{q},\omega)$ ($J(\mathbf{q},\omega)$) at $\omega = -10meV$. From top to bottom, the rows correspond to temperatures $T = 0.1, 0.9$, and $1.1T_c$. For $T = 0.1T_c$ all octet vectors can be identified in the contour plots. As the temperature is increased and non-condensed pairs (with non-vanishing γ) replace the coherent superconducting pairs, the intensity of the peaks rapidly reduces in both spectroscopies. The intensity of

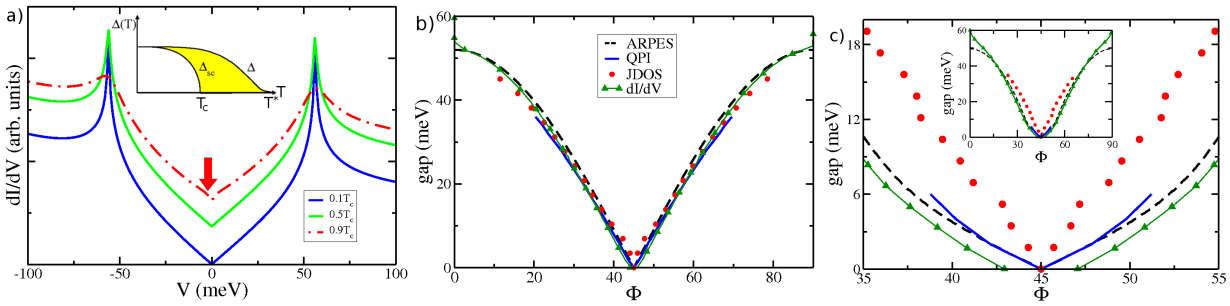

Figure 2: (Color online) Analysis of the moderately underdoped case. The excitation gap Δ and order parameter Δ_{sc} are equivalent at $T = 0$. (a) The differential conductance at $T = 0.1, 0.5$, and $0.9T_c$. The arrow identifies a slight "kink" or inflection point in the conductance. The inset shows the temperature dependencies of Δ and Δ_{sc}, where the shaded area indicates the size of Δ_{pg} that contributes to the full gap. (b)The four spectroscopic gaps extracted at $T = 0.1T_c$.(c)Nodal region of the extracted gaps at $T = 0.9T_c$, where various spectroscopies yield differently shaped gaps. The inset show the full range of the gaps.

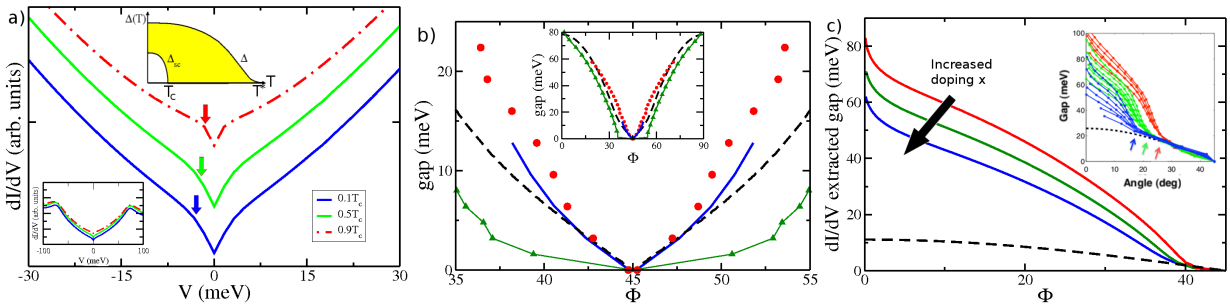

Figure 3: (Color online) Analysis of the heavily underdoped case. (a)The differential conductance at temperatures $T = 0.1, 0.5$, and $0.9T_c$. The arrows indicate kinks in the gap. The lower left inset is the full range of the differential conductances. The centered inset shows the temperature dependences of Δ and Δ_{sc} in the heavily underdoped model. (b)Extracted gaps in the heavily underdoped model at $T = 0.1T_c$. Different spectral gaps are labeled identically as those in Fig. 2 (b). (c) Differential conductances at three different dopings, with inset showing the counterpart data[4]. The dashed curve is a d-wave fit to the nodal regime.

the octet vectors eventually vanishes above T_c, signaling the breakdown of the superconducting state. There is a key distinction between the $\delta n(\mathbf{q}, \omega)$ and $J(\mathbf{q}, \omega)$. The analysis of $\delta n(\mathbf{q}, \omega)$[19] shows an extinction point (the energy above which the octet vectors are no longer consistent) that scales with the order parameter, Δ_{sc}, and thus terminates at T_c. It should be noted that this result appears to differ with some recent experiments on heavily underdoped cuprates[2,3] associating the QPI extinction with the antiferromagnetic zone boundary and finding an, albeit greatly reduced, QPI signal above T_c. This latter, controversial[20], point does not appear[21] to apply to the moderately underdoped cuprates. In contrast, the octet vectors in $J(\mathbf{q}, \omega)$ are more robust and persist to energies comparable to the total gap ($\approx 0.8\Delta$). A small trace of the $J(\mathbf{q}, \omega)$ octet vectors is found above T_c, but the peaks are substantially broadened and the octet inversion is problematic, as is consistent with some experimental claims[8].

In Fig. 2(a) we plot the differential conductance at three different temperatures ($T = 0.1, 0.5$, and $0.9T_c$) in the moderately underdoped system. At the lowest temperature $T = 0.1T_c$, the behavior is characteristic of a simple $d_{x^2-y^2}$-wave gap. As the number of non-condensed pairs increase with increasing temperature, the coherence peaks broaden. The red arrow denotes a slight kink in the shape of the dI/dV spectrum which appears near T_c. The inset plots the temperature dependence of the superconducting gap, Δ_{sc}, which vanishes at T_c, and total gap Δ, which persists up to T^*. A collection of the extracted gaps for $T = 0.1T_c$ in Fig.2(b) shows that they are in good quantitative agreement over a wide range of angle Φ. However, the gaps obtained from $\delta n(\mathbf{q}, \omega)$ and $J(\mathbf{q}, \omega)$ exhibit different extinction energies near 35 and $45meV$, respectively. In contrast, for $T = 0.9T_c$, the agreement between the various gaps breaks down, primarily in the nodal region, as shown in Fig.2(c). Except for $J(\mathbf{q}, \omega)$, all gaps show a suppression in the nodal region associated with the diminishing Δ_{sc}, with the largest suppression found in the gap extracted from the dI/dV fit. This behavior is associated with the low energy part of the dI/dV curve, where the slope, for $V \approx -3$ to $3meV$ is larger than elsewhere, resulting in a smaller gap.

We note that the discrepancies between these four spectral gaps scale with the deviation of the gap from a pure $d_{x^2-y^2}$-form. These gap deviations at high temperatures below T_c are not unexpected in view of the second order phase transition and the presence of Fermi arcs above T_c[14]. Indeed, this smooth evolution with decreasing T of the ARPES spectral gap from a Fermi arc shape first to a distorted d-wave (near T_c) and then to a simple d-wave ground state has been reported[6,14] for moderately underdoped cuprates. At a microscopic level,

these deviations from a simple d-wave are associated with the relatively small size of Δ_{sc}/Δ.

In developing a model for the strongly underdoped cuprates, we were guided two experimental observations at $T \ll T_c$: (i) the dI/dV and ARPES - derived nodal gaps show a strong suppression[4,6], and (ii) the differential conductances exhibit inflection points (kinks)[4]. The results suggest that both observations can be explained within our theoretical scenario if one assumes that even in the limit $T \to 0$, an appreciable fraction of non-condensed pairs is present, perhaps due to a contamination from the insulating phase. A schematic temperature dependence of the total gap, Δ and the order parameter Δ_{sc} is shown in the lower left inset of Fig. 3 (a). For concreteness, we take $\Delta_{sc}(0)/\Delta_{pg}(0) = 0.5$; the details of the temperature evolution of the gaps are outlined in Ref. 15. The resulting differential conductance for three different temperatures ($T = 0.1, 0.5$, and $0.9T_c$) is shown in Fig. 3(a). The lower right inset plots the frequency dependence of dI/dV over a wider range.

In Fig. 3 (b), we present the spectral gaps extracted from the four spectroscopic techniques for $T = 0.1T_c$. We again observe that the deviation of the gap from a pure $d_{x^2-y^2}$-form coincides with significant discrepancies between these four spectral gaps. The nodal region, shown in the main figure emphasizes *the clear similarity between the gaps extracted from the low temperature heavily underdoped model (Fig.3(b)) and those near T_c in the moderately underdoped samples (Fig.2(c))*. The gaps over the full range of angles are shown in the inset. Finally, in Fig. 3 (c) we present the evolution of dI/dV with doping, which was experimentally investigated in Ref.4 (see inset). Here, we hold the $T = 0$ superconducting gap Δ_{sc} constant while the zero temperature pseudogap Δ_{pg} is taken to increase as the doping is decreased, thereby leading to an increased total gap Δ with underdoping, as experimentally observed. In accord with experiment[4], there is universal behavior near $V = 0$ associated with the superconducting contribution while the spectra for the lowest (highest) doping breaks away from the universal curve at the smallest (highest) Φ.

Past work in the literature[7,8,9] generally builds on the premise that there is universality in the spectral gap measurements. In Ref. 22 good agreement was reported between $\delta n(\mathbf{q}, \omega)$ and $J(\mathbf{q}, \omega)$ (albeit in a case where there are no deviations from the pure d-wave gap shape). In Ref. 7 it was presumed that coherence established in ARPES experiments near the antinodes would reflect on the extinction point found in QPI, and that such extinction was difficult to understand without invoking specific impurity models. By contrast, in this paper we have addressed four different spectroscopic probes in one theoretical framework and shown how disparate the results are, except in the limiting case of low T moderately underdoped cuprates. Another important conclusion of the present approach is that it is sufficient to presume a smooth evolution of the spectral gaps with doping x and temperature T in order to understand the heavily underdoped cuprates; introduction of a quantum critical point or competing order is not necessary.

This work was supported by Grant Nos. NSF PHY-0555325 and NSF-MRSEC DMR-0213745 and by the U.S. Department of Energy under Award No. DE-FG02-05ER46225 (D.M.). We thank A. Yazdani and C. Parker and M. Hashimoto for their help and advice.

[1] S. Hufner, M. A. Hossain, A. Damascelli, and G. Sawatzky, Rep. Prog. Phys. **71**, 062501 (2008), and references therein.

[2] Y. Kohsaka, C. Taylor, P. Wahl, A. Schmidt, J. Lee, K. Fujita, J. Alldredge, K. McElroy, J. Lee, H. Eisaki, et al., Nature **454**, 1072 (2008).

[3] J. Lee, K. Fujita, A. R. Schmidt, C. K. Kim, H. Eisaki, S. Uchida, and J. C. Davis, Science **325**, 1099 (2009).

[4] A. Pushp, C. Parker, A. Pasupathy, K. Gomes, S. Ono, J. Wen, Z. Xu, G. Gu, and A. Yazdani, Science **324**, 1689 (2009).

[5] T. Kondo, R. Khasanov, T. Takeuchi, J. Schmalian, and A. Kaminski, Nature **457**, 296 (2009).

[6] W. S. Lee, I. M. Vishik, K. Tanaka, D. H. Lu, T. Sasagawa, N. Nagaosa, T. P. Devereaux, Z. Hussain, and Z. X. Shen, Nature **450**, 81 (2007).

[7] I. M. Vishik, E. A. Nowadnick, W. S. Lee, Z. X. Shen, B. Moritz, T. P. Devereaux, K. Tanaka, T. Sasagawa, and T. Fujii, Nature Physics **5**, 718 (2009).

[8] U. Chatterjee, M. Shi, A. Kaminski, A. Kanigel, F. H. M, K. Terashima, T. Takahashi, S. Rosenkranz, Z. Z. Li, H. Raffy, et al., Phys. Rev. Lett. **96**, 107006 (2006).

[9] K. McElroy, R. W. Simmonds, J. E. Hoffman, D. H. Lee, J. Orenstein, H. Eisaki, S. Uchida, and J. C. Davis, Nature **422**, 592 (2003).

[10] T. Hanaguri, Y. Kohsaka, J. C. Davis, C. Lupien, I. Yamada, M. Azuma, M. Takano, K. Ohishi, M. Ono, and H. Takagi, Nature Phys. **3**, 865 (2007).

[11] Q. J. Chen, J. Stajic, S. Tan, and K. Levin, Phys. Rep. **412**, 1 (2005).

[12] K. Tanaka, W. S. Lee, L. D. H, A. Fujimori, T. Fujii, I. Terasaki, D. J. Scalapino, T. P. Devereaux, Z. Hussain, and Z. X. Shen, Science **314**, 1910 (2006).

[13] T. Kondo, T. Takeuchi, A. Kaminski, S. Tsuda, and S. Shin, PRL **98**, 267004 (2007).

[14] A. Kanigel, U. Chatterjee, M. Randeria, M. R. Norman, S. Souma, M. Shi, Z. Z. Li, H. Raffy, and J. C. Campuzano, Phys. Rev. Lett. **99**, 157001 (2007).

[15] C. C. Chien, Y. He, Q. J. Chen, and K. Levin, Phys. Rev. B **79**, 214527 (2009).

[16] M. R. Norman, M. Randeria, H. Ding, and J. C. Campuzano, Phys. Rev. B **57**, R11093 (1998).

[17] A. V. Chubukov, M. R. Norman, A. J. Millis, and E. Abrahams, Phys. Rev. B **76**, 180501(R) (2007).

[18] R. Damascelli, Z. Hussain, and Z.-X. Shen, Rev. Mod. Phys. **75**, 473 (2003).

[19] D. Wulin, Y. He, C. C. Chun, D. Morr, and K. Levin, Phys. Rev. B **80**, 134504 (2009).

[20] A. Yazdani, Private Communication.

[21] S. Misra, M. Vershinin, P. Philips, and A. Yazdani, Phys. Rev. B **70**, 220503(R) (2004).

[22] K. McElroy, G. H. Gweon, S. Y. Zhou, J. Graf, S. Uchida, H. Eisaki, H. Takagi, T. Sasagawa, D. H. Lee, and A. Lanzara, Phys. Rev. Lett. **96**, 067005 (2006).